

Supporting Information

# Construction of 3D/2D g-C<sub>3</sub>N<sub>4</sub>/ZnIn<sub>2</sub>S<sub>4</sub> hollow spherical heterostructure for efficient CO<sub>2</sub> photoreduction under visible light

Boyu Shao<sup>a</sup>, Junyan Wang<sup>a</sup>, Yizhong Zhang<sup>a</sup>, Xin Tan<sup>a,d</sup>, Wei Zhou<sup>c</sup>, Yiliang Chen<sup>b</sup>, Tao Xie<sup>b</sup>, and Tao Yu<sup>b,e\*</sup>

<sup>a</sup>*School of Environmental Science and Engineering, Tianjin University, Tianjin, 300350, China*

<sup>b</sup>*School of Chemical Engineering and Technology, Tianjin University, Tianjin, 300350, China*

<sup>c</sup>*School of Science, Tianjin University, Tianjin, 300350, China*

<sup>d</sup>*School of Science, Tibet University, Lhasa, 850000, China*

<sup>e</sup>*TJU-NIMS International Collaboration Laboratory, School of Materials Science and Engineering, Tianjin University, Tianjin, 300072, China*

\*Corresponding Author.

E-mail address: [yutao@tju.edu.cn](mailto:yutao@tju.edu.cn) (T. Yu)

## Text S1. Photoelectrochemical measurements

The photoelectrochemical properties were investigated in a three-electrode cell by using CHI660E workstation (Chenghua, Shanghai). The as-synthesized samples coated pretreated indium–tin oxide (ITO) conductor glass, a Pt wire, and a saturated calomel electrode (SCE) and  $\text{Na}_2\text{SO}_4$  (0.1 M) aqueous solution were used as the working electrode, the counter-electrode, the reference electrode, and the electrolyte, respectively. A 500 W Xenon lamp equipped with a 420 nm cutoff filter was utilized as a light source. The photocurrent with ON/OFF cycles was measured at an applied potential of 0.2 V versus SCE, sample interval (s) = 20, run time (sec) = 440, quiet time (sec) = 0, sensitivity (A/V) =  $10^{-6}$ . The electrochemical impedance spectroscopy (EIS) was taken in the frequency range of  $10^6$  – 0.01 Hz at the open circuit potential. To prepare the working electrode, 10 mg of CN, IZIS and IZIS-CN were first dispersed into ethanol (450  $\mu\text{L}$ ) and 50  $\mu\text{L}$  Nafion mixtures using soft ultrasonic stirring to obtain a uniform suspension. The solution containing the samples (30  $\mu\text{L}$ ) was dropped onto the pretreated ITO conductor glass substrate (ca.  $1\times 1\text{ cm}^2$ ), which were then dried in an oven at 60 °C for 3 h.

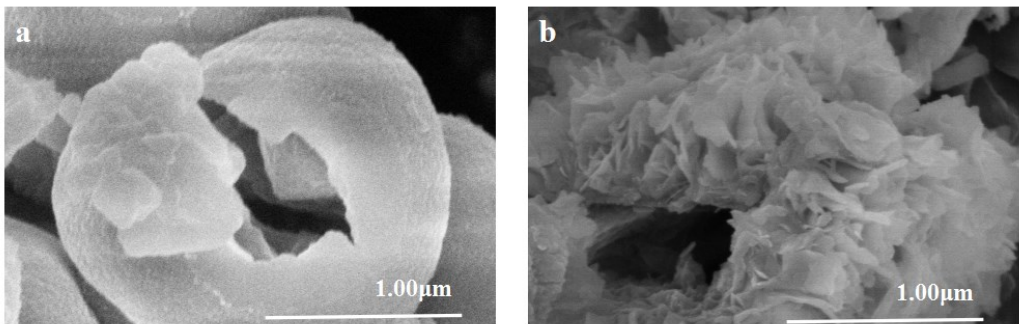


Figure S1. SEM images of (a) CN and (b) IZIS-CN100.

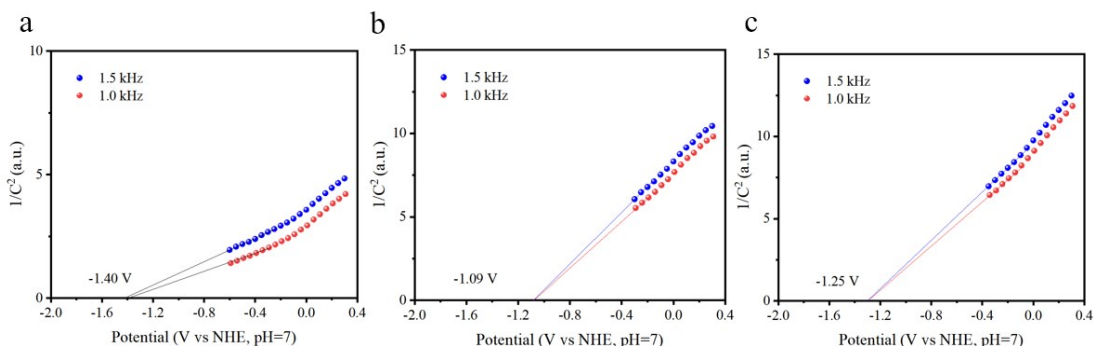


Figure S2. Mott-Schottky plots of (a) CN, (b) IZIS and (c) IZIS-CN100.

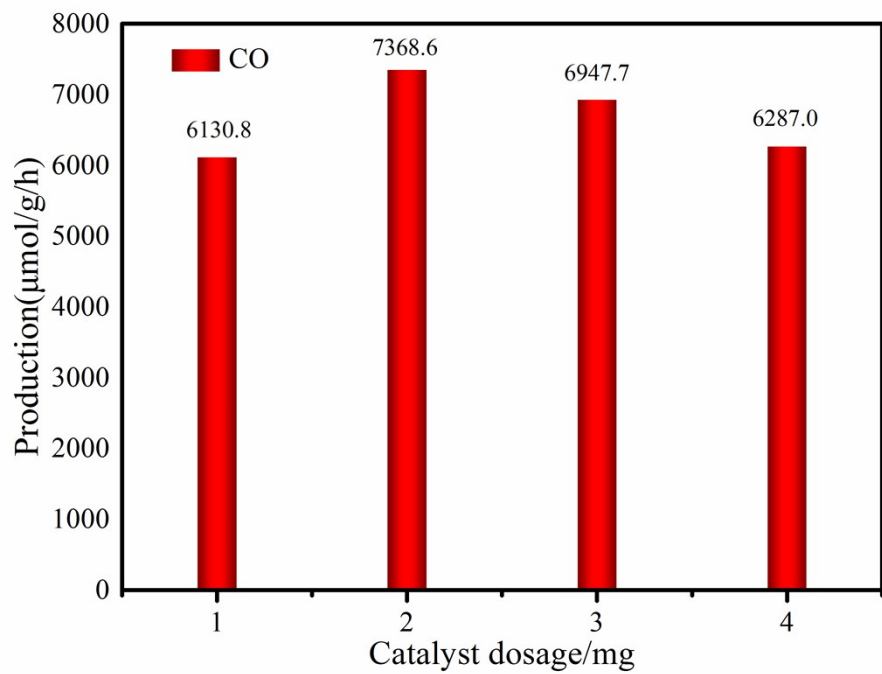


Figure S3. Optimal catalyst dosage of ZIS-CN100

Table S1. Comparison of CO<sub>2</sub> photoreduction performance.

Catalyst	Photosensitizer Cocatalyst	Sacrificial agent	Major product evolution rate (μmol h <sup>-1</sup> g <sup>-1</sup> )	Ref.
ZnIn <sub>2</sub> S <sub>4</sub> -In <sub>2</sub> O <sub>3</sub>	/	TEOA	CO: 3075	1
	Co(bpy) <sub>3</sub> <sup>2+</sup>			
BCN	/	TEOA	CO: 94	2
	Co(bpy) <sub>3</sub> <sup>2+</sup>			
HR-CN	/	TEOA	CO: 297	3
	Co(bpy) <sub>3</sub> <sup>2+</sup>			
SrTiO <sub>3</sub> /TiO <sub>2</sub>	/	N <sub>2</sub> H <sub>4</sub> ·H <sub>2</sub> O	hydrocarbon: 725.4	4
	Au-Cu			
RuRu'/mpg-C <sub>3</sub> N <sub>4</sub>	/	EDTA·2Na	HCOO <sup>-</sup> : 2011	5
	Ag			
RuRu'/NS-C <sub>3</sub> N <sub>4</sub>	/	EDTA·2Na	HCOO <sup>-</sup> : 57.5	6
	Ag			
C <sub>3</sub> N <sub>4</sub>	/	TEOA	HCOO <sup>-</sup> : 1100	7
	RuP			
Co <sub>3</sub> O <sub>4</sub>	/	TEOA	CO: 2003	8
	Ru(bpy) <sub>3</sub> <sup>2+</sup>			
N-Ta <sub>2</sub> O <sub>5</sub>	/	TEOA	HCOOH: 70	9
	[Ru(dcbpy) <sub>2</sub> (CO) <sub>2</sub> ] <sup>2+</sup>			
MOF-525-Co	/	TEOA	CO: 200.6	10
	/			
UiO-66/CNNS	/	TEOA	CO: 9.79	11
	/			
NH <sub>2</sub> -MIL-125(Ti)	/	TEOA	HCOO <sup>-</sup> : 40	12
	/			
PCN-222	/	TEOA	COOH <sup>-</sup> : 125	13
	/			

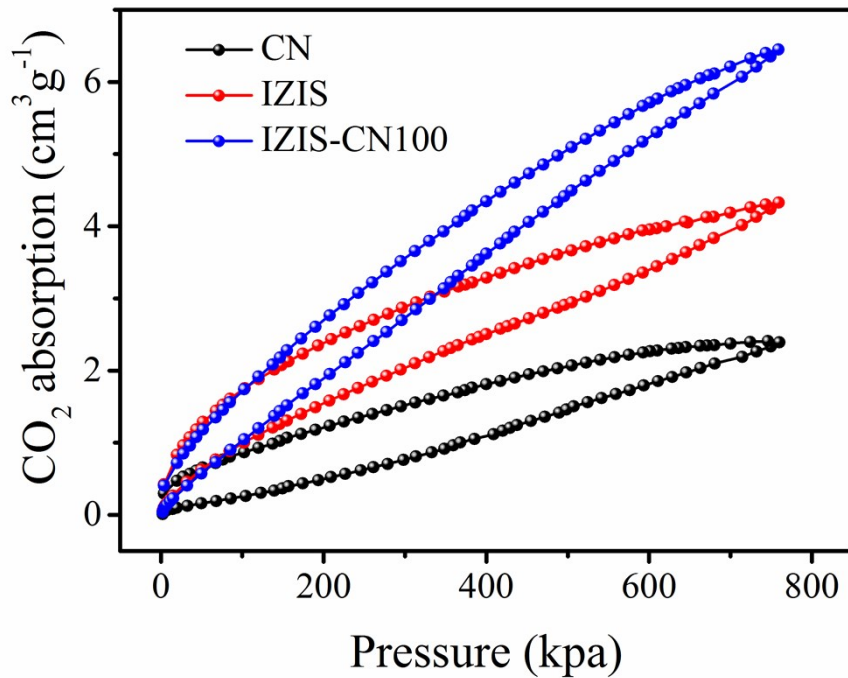


Figure S4. CO<sub>2</sub> adsorption and desorption isotherm of CN, IZIS and IZIS-CN100.

In addition, we performed an equivalent circuit fitting and calculated the internal resistance of the electrode through ZSimpWin. The results are as follows:

Table S2. Fitting parameters values of EIS measurement.

Sample	R <sub>1</sub> (KΩ)	C (KF)
CN	23.47	1.79
IZIS	6.227	1.506
IZIS-CN75	4.333	1.084
IZIS-CN100	1.426	1.472
IZIS-CN125	2.837	1.499

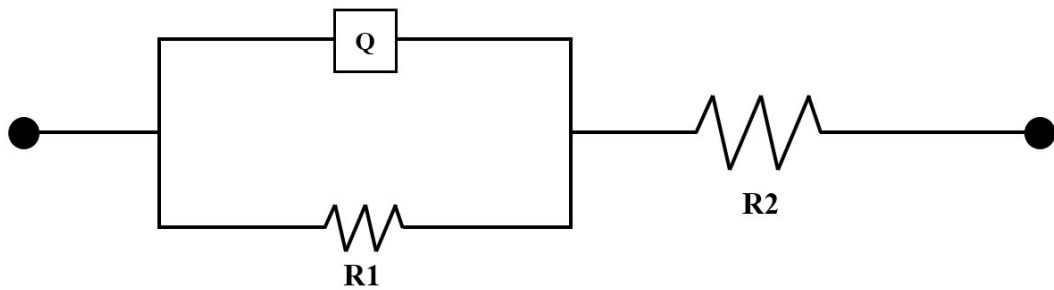


Figure S5. Equivalent circuit diagram of EIS.

## Text S2. Computational details

All calculations here were carried out with the VASP based on density functional theory (DFT). The projector augmented wave (PAW) pseudopotentials and the generalized gradient approximation (GGA) with the Perdew-Burke-Ernzerhof (PBE) functional were employed in the calculations. The wave-functions were expanded by plane-wave with a cutoff energy of 450 eV, and the energy and force convergence threshold were set to 10<sup>-5</sup> eV and 10<sup>-2</sup> eV Å<sup>-1</sup>, respectively. The 3 × 3 × 1 Monkhorst-Pack k-points mesh was adopted for the supercell model with 44 atoms. The conduction band edge and the valence band edge of a semiconductor can be calculated by the following equation :

$$E_{CB} = X - E_c - 0.5E_g$$

$$E_{VB} = E_g - E_{CB}$$

Table S3. The calculated band structures of  $\text{ZnIn}_2\text{S}_4$  and  $\text{g-C}_3\text{N}_4$ .

Sample	$E_g$ (eV)	CB (eV)	VB (eV)
$\text{ZnIn}_2\text{S}_4$	2.18	-0.81	1.37
$\text{g-C}_3\text{N}_4$	2.61	-1.19	1.42

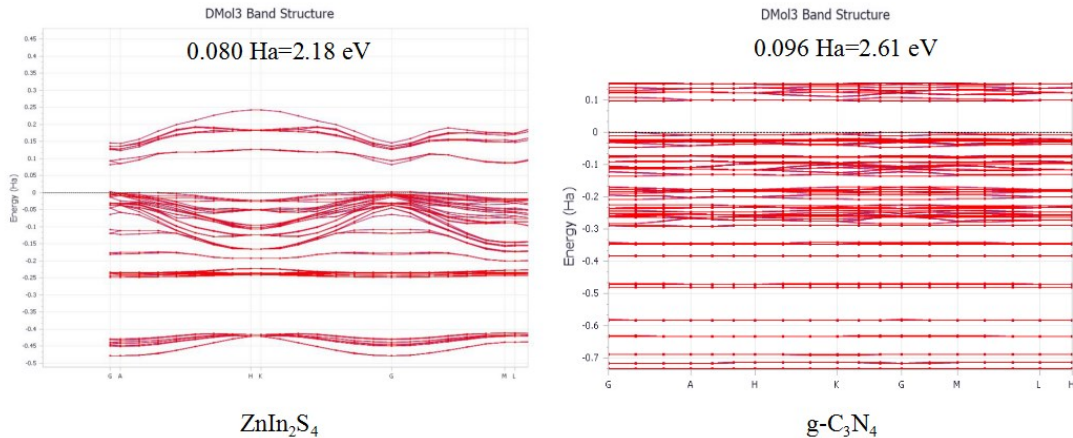


Figure S6. The calculated band structures of  $\text{ZnIn}_2\text{S}_4$  and  $\text{g-C}_3\text{N}_4$  spinels using mBJ potential.

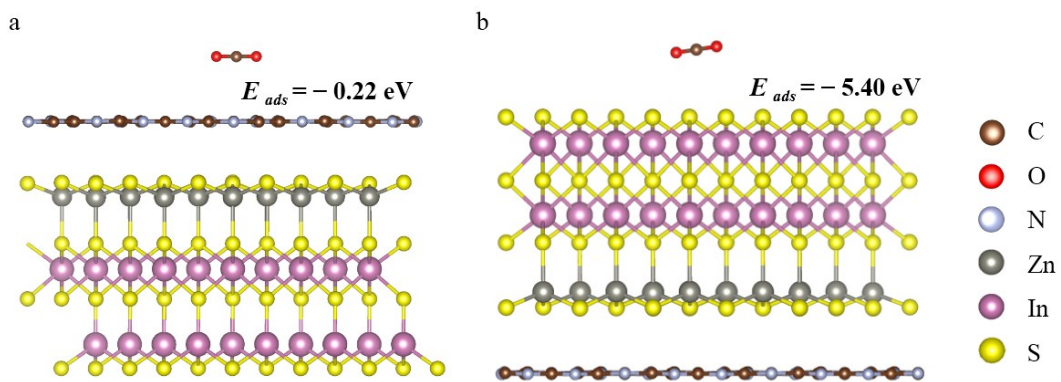


Figure S7.  $\text{CO}_2$  adsorption energy of (a)  $\text{g-C}_3\text{N}_4$  and (b)  $\text{ZnIn}_2\text{S}_4$ .

## References

- 1 S. Wang, B. Y. Guan and X. W. D. Lou, *J Am Chem Soc*, 2018, 140, 5037-5040.
- 2 Huang, C.; Chen, C.; Zhang, M.; Lin, L.; Ye, X.; Lin, S.; Antonietti, M.; Wang, X. *Nat. Commun.* 2015, 6, 7698.
- 3 Zheng, Y.; Lin, L.; Ye, X.; Guo, F.; Wang, X. *Angew. Chem. Int. Ed.* 2014, 53, 11926.
- 4 Kang, Q.; Wang, T.; Li, P.; Liu, L.; Chang, K.; Li, M.; Ye, J. *Angew. Chem. Int. Ed.* 2015, 54, 841.
- 5 Kuriki, R.; Matsunaga, H.; Nakashima, T.; Wada, K.; Yamakata, A.; Ishitani, O.; Maeda, K. *J. Am. Chem. Soc.* 2016, 138, 5159.
- 6 Kuriki, R.; Yamamoto, M.; Higuchi, K.; Yamamoto, Y.; Akatsuka, M.; Lu, D.; Yagi, S.; Yoshida, T.; Ishitani, O.; Maeda, K. *Angew. Chem. Int. Ed.* 2017, 56, 4867.
- 7 Kuriki, R.; Sekizawa, K.; Ishitani, O.; Maeda, K. *Angew. Chem. Int. Ed.* 2015, 54, 2406.
- 8 Gao, C.; Meng, Q.; Zhao, K.; Yin, H.; Wang, D.; Guo, J.; Zhao, S.; Chang, L.; He, M.; Li, Q.; Zhao, H.; Huang, X.; Guo, Y.; Tang, Z. *Adv. Mater.* 2016, 28, 6485.
- 9 Sato, S.; Morikawa, T.; Saeki, S.; Kajino, T.; Motohiro, T. *Angew. Chem. Int. Ed.* 2010, 49, 5101.
- 10 Zhang, H.; Wei, J.; Dong, J.; Liu, G.; Shi, L.; An, P.; Zhao, G.; Kong, J.; Wang, X.; Meng, X.; Zhang, J.; Ye, J. *Angew. Chem. Int. Ed.* 2016, 55, 14310.
- 11 Shi, L.; Wang, T.; Zhang, H.; Chang, K.; Ye, J. *Adv. Funct. Mater.* 2015, 25, 5360.
- 12 Fu, Y.; Sun, D.; Chen, Y.; Huang, R.; Ding, Z.; Fu, X.; Li, Z. *Angew. Chem. Int. Ed.* 2012, 51, 3364.
- 13 Xu, H. Q.; Hu, J.; Wang, D.; Li, Z.; Zhang, Q.; Luo, Y.; Yu, S. H.; Jiang, H. L. *J. Am. Chem. Soc.* 2015, 137, 13440.